

Melting the Superconducting State in the Electron Doped Cuprate $\text{Pr}_{1.85}\text{Ce}_{0.15}\text{CuO}_{4-\delta}$ with Intense near-infrared and Terahertz Pulses

M. Beck,¹ M. Klammer,¹ I. Rousseau,¹ M. Obergfell,^{1,2} P. Leiderer,¹ M. Helm,^{3,4}

V.V. Kabanov,⁵ I. Diamant,⁶ A. Rabinowicz,⁶ Y. Dagan,⁶ and J. Demsar^{1,2}

¹*Dept. of Physics and Center for Applied Photonics, Univ. of Konstanz, D-78457, Germany*

²*Institute of Physics, Johannes Gutenberg-University Mainz, 55128 Mainz, Germany*

³*Institute of Ion Beam Physics and Materials Research,*

Helmholtz-Zentrum Dresden-Rossendorf, P.O. Box 510119, 01314 Dresden, Germany

⁴*Technische Universität Dresden, 01062 Dresden, Germany*

⁵*Jozef Stefan Institute, Ljubljana, SI-1000, Slovenia and*

⁶*Raymond and Beverly Sackler School of Physics and Astronomy, Tel Aviv University, Tel Aviv, 69978, Israel*

We studied the superconducting (SC) state depletion process in an electron doped cuprate $\text{Pr}_{1.85}\text{Ce}_{0.15}\text{CuO}_{4-\delta}$ by pumping with near-infrared (NIR) and narrow-band THz pulses. When pumping with THz pulses tuned just above the SC gap, we find the absorbed energy density required to deplete superconductivity, A_{dep} , matches the thermodynamic condensation energy. Contrary, by NIR pumping A_{dep} is an order of magnitude higher, despite the fact that the SC gap is much smaller than the energy of relevant bosonic excitations. The result implies that only a small subset of bosons contribute to pairing.

PACS numbers: 74.40.Gh, 78.47.J-, 78.47.D-, 74.72.-h

The quest for a pairing boson in cuprate high-temperature superconductors has been one of the key topics of solid state physics ever since the discovery of superconductivity in the cuprates. Recently, numerous femtosecond (fs) real-time studies of carrier dynamics in high- T_c superconductors have been performed aiming to find the coupling strengths between the electrons and other degrees of freedom (high and low frequency phonons, spin fluctuations, electronic continuum)[1–8]. In this approach, fs optical pulses are used to excite the electronic system, while the resulting dynamics are probed by measuring the changes in optical constants [2–6] or the electronic distribution near the Fermi energy [1, 7, 8]. To connect the measured relaxation timescales to the electron-boson coupling strengths, the multi-temperature models are commonly used [9, 10]. These are based on the premise that the electron-electron ($e-e$) thermalization is much faster than the electron-boson relaxation. While these models are commonly used to extract e.g. the electron-phonon ($e-ph$) coupling strengths, numerous inconsistencies have been noted (even for the case of simple metals) [11–14]. An alternative time-domain approach, based on the dynamics in the superconducting state, has been put forward [15, 16]. Under the assumption that the absorbed optical energy is distributed between quasiparticles and high frequency ($\hbar\omega > 2\Delta$) bosons on the sub-picosecond timescale, and taking into account the nonlinearity of relaxation processes (pairwise recombination of quasiparticles), the electron-boson coupling strength is determined by studying the excitation density dependence of the Cooper pair-breaking process [15, 16]. While this approach has been successfully applied to conventional superconductors [16, 17], the results on cuprates show that the energy

density required to suppress superconductivity exceeds the thermodynamic condensation energy, E_c , by an order of magnitude [2, 18–20]. Therefore, the assumption that the absorbed energy is distributed between QPs and the coupled high frequency bosons fails. Considering the possible energy relaxation pathways, this discrepancy in the hole-doped high- T_c cuprates has been attributed to the fact that the superconducting gap, 2Δ , lies well in the range of optical phonons [19]. It has been argued that $\approx 90\%$ of the absorbed energy is directly released to $\hbar\omega < 2\Delta$ modes via rapid $e-ph$ scattering (mainly to sub-gap zone center optical phonons and zone-edge acoustic phonons) and only $\approx 10\%$ is available for condensate quenching [19]. Indeed, it has been shown that in YBCO the rapid $e-ph$ transfer gives rise to a rapid heating of specific phonons on the timescale of ≈ 100 fs [21]. Studying cuprate superconductors with 2Δ far below the energy of optical phonons can put this argument to the test.

In this Letter we present a systematic study of light induced quenching of superconductivity in an e-doped cuprate [22] superconductor $\text{Pr}_{1.85}\text{Ce}_{0.15}\text{CuO}_{4-\delta}$ (PCCO) at optimal doping. We used near-infrared ($\lambda = 800$ nm) as well as narrow-band THz ($\lambda = 144\ \mu\text{m}$) excitation, while probing the superconducting gap dynamics with THz probe pulses. In PCCO $2\Delta \approx 7$ meV [23–26], well below the acoustic phonon cut-off frequency of ≈ 20 meV [27], as well as the energy of the collective electronic mode of $\approx 11 \pm 2$ meV [28, 29]. Like in NbN [16], we expected the absorbed energy density required to deplete superconductivity, A_{dep} , to be in the low temperature limit the same in the two configurations, with $A_{dep} \approx E_c$. We demonstrate that this is not the case, suggesting that the Eliashberg electron-boson coupling

function in cuprates depends strongly on the electron energy, unlike to what is commonly assumed [10, 30].

Optimally doped c-axis oriented PCCO thin films with a thickness $d = 60$ nm were epitaxially grown on LaSrGaO_4 (001) (LSGO) substrates using pulsed laser deposition [31]. Inductive measurements of the samples yield a $T_c \approx 21$ K. The broadband linear and time-resolved THz spectroscopy were performed on the set-up built around a 250 kHz amplified Ti:sapphire laser system and utilizing large area interdigitated photoconductive emitter for the generation of THz pulses [32]. Narrow band THz pumping experiments were performed at the free electron laser (FEL) facility at the Helmholtz-Zentrum Dresden-Rossendorf. Here, intense narrowband (spectral width ≈ 30 GHz, pulse length $\tau_{\text{FEL}} \approx 18$ ps) THz pulses at $\nu_{\text{FEL}} = 2.08$ THz, slightly above the low-temperature gap frequency $2\Delta/\hbar \approx 1.7$ THz [23, 24], were used as both pump and probe sources using the configuration described in Ref.[33].

The equilibrium THz conductivity studies were performed by recording the THz electric fields transmitted through the sample (film on substrate), $E_{tr}(t')$, and the reference (bare substrate), $E_{re}(t')$, using the Pockels effect in GaP. The bandwidth was limited to below 2.5 THz by the TO-Phonon of the LSGO. The complex optical conductivity $\sigma(\omega) = \sigma_1(\omega) + i\sigma_2(\omega)$ was obtained [34] using the Fresnel equations. The normal state $\sigma(\omega)$ can be well approximated by the Drude model, giving the plasma frequency $\nu_p = 190$ THz and the scattering rate $\tau^{-1} = 2.2$ THz, in good agreement with infrared studies on thick films [25, 26]. To estimate the magnitude of 2Δ , we follow the approach of Ref.[26], where 2Δ was extracted from the reflectivity, by reading out the position in the reflectance spectra, below which the reflectivity starts to rise steeply above its normal state value. To do so, we used the measured $\sigma(\omega, T)$, calculated the corresponding bulk reflectivity $R(\omega, T)$, and plot $R(\omega, T) - R(\omega, 30 \text{ K})$, as shown in Fig. 1(d). It follows that the maximum gap frequency $2\Delta/\hbar \approx 1.7$ THz ($\Delta = 3.5$ meV), in good agreement with other studies on c-axis films [23, 26]. Unlike in the BCS case [16], 2Δ displays only weak T-dependence.

In optical-pump – THz probe experiments, the film is excited by a 50 fs near-infrared (NIR) pump pulse centered at 800 nm. The transient spectral conductivity $\sigma(\omega, t_d)$ was measured as a function of time delay t_d between the pump and the THz probe pulse. The quenching of the SC state is found to proceed on a timescale of several ps, while the SC state recovery was on a timescale of 100's of ps. For time delays t_d longer than the characteristic e-e and e-ph thermalization times (both on the order of 1 ps) we find that the measured $\sigma(\omega, t_d)$ can be matched to the equilibrium $\sigma(\omega)$ recorded at a specific temperature T^* [34], i.e. $\sigma(\omega, t_d) \approx \sigma(\omega, T^*)$. This is consistent with the so called T^* -model, where in non-equilibrium the population of QPs, Cooper pairs

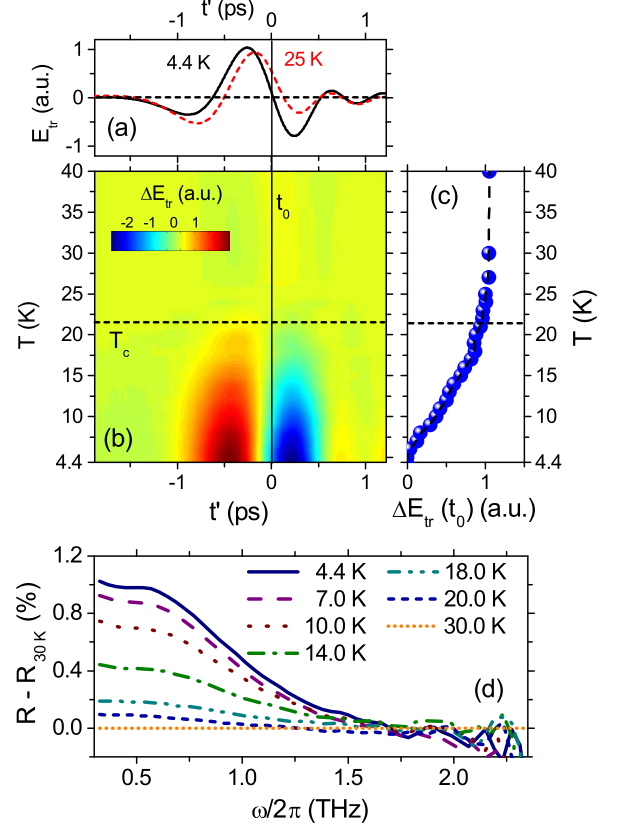


FIG. 1: (color online) Temperature dependence of transmitted THz electric field transients. Panel (a) shows $E_{tr}(t')$ in the normal and superconducting states. The pronounced phase shift is characteristic of the inductive response below T_c . Panel (b) presents $\Delta E_{tr}(T, t') = E_{tr}(T, t') - E_{tr}(25 \text{ K}, t')$, while (c) shows the temperature dependence of $\Delta E_{tr}(T, t_0) = E_{tr}(T, t_0) - E_{tr}(4.4 \text{ K}, t_0)$. Panel (d) presents the temperature dependence of the bulk reflectivity extracted from $\sigma(\omega)$ [34].

and high-frequency ($\hbar\omega > 2\Delta$) bosons are in a quasi-equilibrium at a temperature T^* , which is larger than the base temperature T of $\hbar\omega < 2\Delta$ modes.

To study the excitation density dependence of the SC state dynamics over large range of excitation densities we recorded the induced changes in the transmitted THz electric field at a fixed $t' = t_0$ as a function of t_d , $\Delta E_{tr}(t_0, t_d)$, as in Ref. [16]. As shown in Fig. 1(a)-(c) the transmitted electric field $E_{tr}(t')$ depends strongly on temperature. In particular, for the chosen t_0 - see Fig. 1 - $E_{tr}(t_0, T)$ shows a linear T-dependence over a large T-range below T_c .

Figure 2(a) shows the recorded $\Delta E_{tr}(t_0, t_d)$ transients for $T = 4.4$ K and a set of absorbed optical energy densities A^{NIR} (in mJ/cm^2). Here, A^{NIR} is extracted from the incoming laser pulse fluence and the absorption coefficient of PCCO at 800 nm, which we have measured. It follows from the data that both, SC state de-

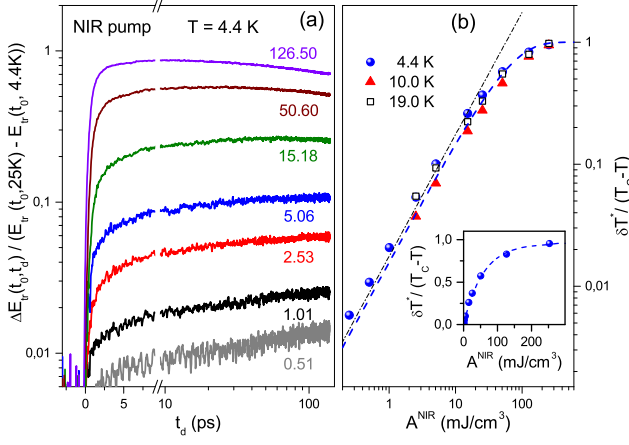


FIG. 2: (color online) (a) Transient changes of the transmitted THz electric field $\Delta E_{tr}(t_0, t_d)$, recorded at 4.4 K for different absorbed energy densities A^{NIR} in mJ/cm^3 . The curves are normalized to the change in $E_{tr}(t_0)$ between 4.4 K and 25 K (above T_c). (b) Maximum increase in effective temperature, δT^* , as a function of A^{NIR} for three base temperatures, normalized to the respective maximum change in T^* , i.e. $T_c - T$. The dashed (blue) line presents the saturation model fit, while the dotted line presents the linear extrapolation. Inset presents the 4.4 K data on a linear scale.

pletion and recovery depend on excitation density. Similar observations have been made on MgB_2 [17] and NbN [16], and could be well accounted by the phenomenological Rothwarf-Taylor model [15]. In particular, the slow timescale for depletion of the SC state (for lowest excitation densities several 10s of ps!) and its excitation density dependence can be attributed to Cooper pair-breaking by $\hbar\omega > 2\Delta$ bosons generated during the relaxation of high energy quasiparticles towards the gap [15–17].

Here, we focus on the energetics of the SC state depletion. We chose $\Delta E_{tr}(t_0, t_d = 30 \text{ ps})$ to determine the change in effective temperature T^* as a function of excitation density. The link to T^* is provided by the T-dependence of $\Delta E_{tr}(t_0, T)$ in equilibrium shown in Fig. 1(c); we used linear interpolation for low excitation densities. The relative change in T^* , $\delta T^*/(T_c - T)$, as a function of A^{NIR} is shown in Fig. 2(b). For low A^{NIR} the induced changes scale with A^{NIR} , yet showing the expected saturation at high densities. By applying a simple saturation model fit, where $\frac{\delta T^*}{T_c - T} = 1 - \exp(-A^{NIR}/A_{dep}^{NIR})$, we extract the absorbed energy density required for depleting the SC state, A_{dep}^{NIR} . At 4.4 K we find $A_{dep}^{NIR} \approx 60 \text{ mJ}/\text{cm}^3$, comparable to the value obtained on $\text{Nd}_{1.85}\text{Ce}_{0.15}\text{CuO}_{4+\delta}$ [35]. This energy is 6 times the superconducting state condensation energy of PCCO, $E_c \simeq 10 \text{ mJ}/\text{cm}^3$ [36], following the trend of hole-doped cuprates where $A_{dep}^{NIR} \gg E_c$ [2, 19, 20, 35]. We note that A_{dep}^{NIR} is substantially lower than the energy needed to thermally suppress superconductivity given by $E_{th} = \int_{4.4\text{K}}^{21\text{K}} C_p(T) dT \simeq 250 \text{ mJ}/\text{cm}^3$, where $C_p(T)$ is

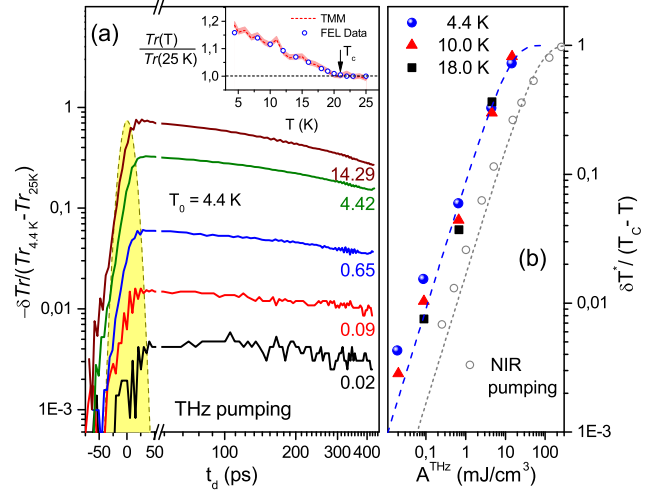


FIG. 3: (color online) (a) The changes in the THz transmission intensity δTr after photoexcitation with intense THz pulses at $T = 4.4 \text{ K}$ (absorbed energy densities A^{THz} in mJ/cm^3 are listed). The shaded area presents the cross-correlation of narrow-band THz pulses. Inset shows the T-dependence of equilibrium Tr . The measured transmission in the FEL set-up matches well the TMM calculation based on the measured $\sigma(\omega)$. (b) The change in effective temperature δT^* as a function of A^{THz} for three base temperatures. Dashed blue line is the fit with simple saturation model. Open (grey) circles and the dotted (grey) line present the data obtained by NIR pumping for comparison.

the total specific heat [36].

We further studied the SC state quenching in PCCO using intense THz pulses. This way the electronic system is excited directly, with quasiparticles having small excess energy. A single-color pump probe scheme was used [33]. The T-dependence of transmission intensity (Tr) in equilibrium is shown in inset to Fig. 3(a). The measurements agree with the transfer-matrix method (TMM) calculation based on the optical conductivity data obtained by broadband THz spectroscopy [34].

Figure 3(a) presents the time-evolution of the normalized pump-induced changes in transmission (δTr) recorded for several A^{thz} . The shaded area corresponds to the intensity cross-correlation of THz pulses. Unlike in the NIR-pump experiments, no SC state suppression dynamics beyond the THz pump pulse duration is observed, despite the fact that the lowest excitation densities were an order of magnitude lower than in the NIR pump study. This clearly demonstrates different excitation mechanisms. While by pumping with THz photons with $\nu_{FEL} > 2\Delta/\hbar$ Cooper pairs are broken directly, by NIR pumping Cooper pairs are broken mainly by $\hbar\omega > 2\Delta$ bosons generated during the cascade of high energy quasiparticles towards the gap edge.

Assuming the T^* -approximation as for NIR pumping, we convert the maximum induced changes in Tr into

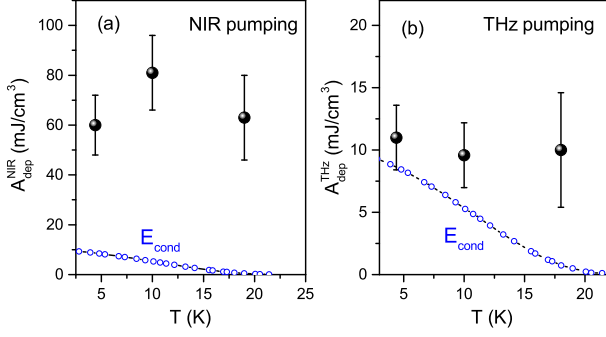


FIG. 4: Comparison of the absorbed optical energy density required for superconducting state depletion for (a) pumping with NIR (1.5 eV) and (b) THz (8.6 meV) pulses.

changes of T^* , using the calibration curve in inset to Fig. 3(a). Figure 3(b) summarizes the results for three different base temperatures, indicating similar values of A_{dep}^{THz} . Contrary to A_{dep}^{NIR} , $A_{dep}^{THz}(4.4\text{ K}) \approx 11\text{ mJ/cm}^3$ is within errorbars identical to E_c . This implies that almost all of the deposited energy is directly used for condensate depletion and only a miniscule amount of energy is transferred into the bosonic system. Since the recovery dynamics is identical for the two excitation processes, and can be attributed to the boson-bottleneck scenario, some energy has to be transferred to the $\hbar\omega > 2\Delta$ bosonic modes. However, due to the detailed balance [15, 17] between the QP density, $n_{qp} \propto \exp(-\Delta/k_B T)$, and the $\hbar\omega > 2\Delta$ boson density, $n_b \propto \exp(-2\Delta/k_B T)$, where $n_b \propto n_{qp}^2$, the energy stored in the latter is negligible for $\Delta > k_B T$.

Figure 4 summarizes the dependence of A_{dep} on the pump photon energy and T . The observation that the low- T value of A_{dep}^{THz} matches E_c is consistent with expectations. Far more surprising is the result of the NIR pumping. Considering the fast condensate depletion times and specific heats of different bosonic subsystems (phonons, spin fluctuations), the observation in hole doped cuprates that $A_{dep}^{NIR} \gg E_c$ was explained by the dominant *e-ph* (pairing) interaction [2]. In this scenario $\hbar\omega > 2\Delta$ phonons couple to the condensate via pair-breaking (and re-pairing), while a large amount of the absorbed energy is rapidly transferred to optical phonons with $\hbar\omega < 2\Delta$ [19, 20]. These act as an effective heat sink, yet lack the energy for breaking up of Cooper pairs. According to this scenario, $A_{dep}^{NIR} \approx E_c$ for superconductors with small Δ [19, 20], as shown for NbN [16] and ferropnictides [20]. Since in PCCO $2\Delta \approx 7\text{ meV}$ is far below the acoustic phonon cut-off energy of $\approx 20\text{ meV}$ [27], this interpretation is hereby challenged. Since $A_{dep}^{NIR} \ll E_{th}$ we can exclude $\hbar\omega < 2\Delta$ acoustic phonons as an effective energy sink during the initial *e-ph* cascade. Consequently, our results suggest a rapid *electron-boson* energy transfer following NIR pumping, yet *only selected modes couple to*

the condensate. We should note that no significant variation of A_{dep} on base temperature is observed. This is not surprising for NIR pumping, where $A_{dep}^{NIR} \gg E_c$, and $\leq 20\%$ of absorbed energy is used for condensate depletion. The fact that similar is observed by THz pumping is puzzling. We speculate that this may be linked to the enhancement of SC due to nonequilibrium electron distribution as observed in NbN [33].

The observation that in PCCO in the low- T limit $A_{dep}^{NIR} \gg A_{dep}^{THz} \approx E_c$ implies, quite generally, that the Eliashberg coupling function strongly depends on the electron energy. The electron-boson spectral function $\alpha^2 F(\varepsilon, \varepsilon', \Omega)$, where ε and ε' are the electronic and Ω the bosonic energy, is commonly approximated by $\alpha^2 F(\varepsilon_F, \varepsilon_F, \Omega) = \alpha^2 F(\Omega)$, since it is customary to assume that its variation on ε and ε' on the energy scale smaller than the electronic bandwidth can be neglected [30]. Our result, that by NIR pumping most of the energy is transferred to bosonic excitations, which at the same time do not couple to the condensate, suggests the failure of the above assumption in cuprates. This implies that $\alpha^2 F$ changes dramatically on the energy scale of (a few) 100 meV.

Considering the possible scenarios of superconductivity being mediated by the phonons or magnetic excitations, the results suggest that high energy electrons strongly couple to phonons (or magnetic modes), while the situation is reversed at low energies. Here, by high energy we refer to $\approx 100\text{ meV}$, since for energies of the order of the NIR photon energy the e-e scattering dominates the e-boson scattering thereby substantially reducing the average electron excess energy on the timescale of a few fs [37]. Presuming the situation is similar in both electron and hole doped cuprates, and taking into account the result that NIR pumping in YBCO results in a rapid e-ph energy transfer [21], this result may suggest that pairing in cuprates is mediated by magnetic excitations. Alternatively, we could assume that high energy electrons emit magnetic excitation on the fs timescale [38]. If so, these nonequilibrium magnetic excitations are almost uncoupled from the condensate and therefore do not act as pair-breakers.

Note that the proposed scenario is based on a very simple observation that the excitations created by the high energy electrons are poorly coupled to the condensate. Therefore the relaxation times due to this coupling is longer than the anharmonic decay of these excitations. As a result Rothwarf and Taylor bottleneck [15] is not operational for these excitations.

In summary, we present photoinduced THz conductivity dynamics in the electron-doped cuprate PCCO, focusing on melting the SC state with both NIR and THz pulses. The absorbed energy density required for SC state depletion, A_{dep} , was found to match the condensation energy when pumping with narrow band THz pulses. With NIR excitation, however, $A_{dep}^{NIR} \gg E_c$, despite the

fact that 2Δ is small compared to relevant bosonic energy scales. The data imply that following NIR pumping a rapid *electron-boson* energy transfer takes place, yet only selected bosonic modes (e.g. antiferromagnetic fluctuations, or specific lattice modes) do couple to the condensate. Further systematic studies, where excitation energy is varied over a large energy range, and supported by theoretical modelling are clearly required in cuprates, as well as in other systems with competing orders.

This work was supported by the German Israeli DIP project No. 563363, Alexander von Humboldt Foundation, Kurt Lion Foundation, Zukunftskolleg and Center for Applied Photonics at the University of Konstanz. We thank P. Michel and the FELBE team for their dedicated support. Y.D. acknowledges support from the Israel Science Foundation under grant 569/13.

-
- [1] L. Perfetti, P.A. Loukakos, M. Lisowski, U. Bovensiepen, H. Eisaki, M. Wolf, *Phys. Rev. Lett.* **99**, 197001 (2007).
 - [2] P. Kusar, V.V. Kabanov, J. Demsar, T. Mertelj, S. Sugai, and D. Mihailovic, *Phys. Rev. Lett.* **101**, 227001 (2008).
 - [3] C. Gadermaier, A. S. Alexandrov, V.V. Kabanov, P. Kusar, T. Mertelj, X. Yao, C. Manzoni, D. Brida, G. Cerullo, and D. Mihailovic, *Phys. Rev. Lett.* **105**, 257001 (2010).
 - [4] S. Dal Conte, C. Giannetti, G. Coslovich, F. Cilento, D. Bossini, T. Abebaw, F. Banfi, G. Ferrini, H. Eisaki, M. Greven, A. Damascelli, D. van der Marel, F. Parmigiani, *Science* **335**, 1600 (2012).
 - [5] B. Mansart, D. Boschetto, A. Savoia, F. Rullier-Albenque, F. Bouquet, E. Papalazarou, A. Forget, D. Colson, A. Rousse, and M. Marsi, *Phys. Rev. B* **82**, 024513 (2010).
 - [6] L. Stojchevska, P. Kusar, T. Mertelj, V. V. Kabanov, X. Lin, G. H. Cao, Z. A. Xu, and D. Mihailovic, *Phys. Rev. B* **82**, 012505 (2010).
 - [7] L. Rettig, R. Cortes, S. Thirupathaiah, P. Gegenwart, H. S. Jeevan, M. Wolf, J. Fink, and U. Bovensiepen, *Phys. Rev. Lett.* **108**, 097002 (2012).
 - [8] C. L. Smallwood, J.P. Hinton, C. Jozwiak, W. Zhang, J.D. Koralek, H. Eisaki, D.-H. Lee, J. Orenstein, A. Lanzara, *Science* **336**, 1137 (2012).
 - [9] M.I. Kaganov, I.M. Lifshitz, L.V. Tantarov, *Zh. Exsp. Theor. Fiz.* **31**, 232 (1956) [*Sov.Phys. JETP* **4**, 173 (1957)].
 - [10] P.B. Allen, *Phys. Rev. Lett.* **59**, 1460 (1987).
 - [11] W.S. Fann, R. Storz, H.W.K. Tom, and J. Bokor, *Phys. Rev. Lett.* **68**, 2834 (1992); *ibid. Phys. Rev. B* **46**, 13592 (1992).
 - [12] R.H.M. Groeneveld, R. Sprik, and A. Lagendijk, *Phys. Rev. B* **51**, 11433 (1995), and references therein.
 - [13] V.V. Kabanov, and A.S. Alexandrov, *Phys. Rev. B* **78**, 174514 (2008).
 - [14] J. Demsar and T. Dekorsy, in *Optical Techniques for Solid-State Materials Characterization*, Edited by R.P. Prasankumar and A.J. Taylor (Francis & Taylor, New York, 2011).
 - [15] V.V. Kabanov, J. Demsar, and D. Mihailovic, *Phys. Rev. Lett.* **95**, 147002 (2005).
 - [16] M. Beck, M. Klammer, S. Lang, P. Leiderer, V.V. Kabanov, G.N. Gol'tsman, and J. Demsar, *Phys. Rev. Lett.* **107**, 177007 (2011).
 - [17] J. Demsar, R.D. Averitt, A. J. Taylor, V. V. Kabanov, W. N. Kang, H. J. Kim, E. M. Choi, and S. I. Lee, *Phys. Rev. Lett.* **91**, 267002 (2003).
 - [18] C. Giannetti, G. Zgrablic, C. Consani, A. Crepaldi, D. Nardi, G. Ferrini, G. Dhalenne, A. Revcolevschi, and F. Parmigiani, *Phys. Rev. B*, **80**, 235129 (2009).
 - [19] M. Beyer, D. Stadtter, M. Beck, H. Schafer, V.V. Kabanov, G. Logvenov, I. Bozovic, G. Koren, and J. Demsar, *Phys. Rev. B* **83**, 214515 (2011).
 - [20] L. Stojchevska, P. Kusar, T. Mertelj, V. V. Kabanov, Y. Toda, X. Yao, and D. Mihailovic, *Phys. Rev. B* **84**, 180507(R) (2011).
 - [21] A. Pashkin, *et al.*, *Phys. Rev. Lett.* **105**, 067001 (2010).
 - [22] N. P. Armitage, P. Fournier, R. L. Greene, *Rev. Mod. Phys.* **82**, 2421 (2010).
 - [23] Y. Dagan, R. Beck and R. Greene, *Phys. Rev. Lett.* **99**, 147004 (2007).
 - [24] I. Diamant, R.L. Greene, Y. Dagan, *Phys. Rev. B* **80**, 012508 (2009).
 - [25] A. Zimmers, R.P.S.M. Lobo, N. Bontemps, C.C. Homes, M.C. Barr, Y. Dagan, and R.L. Greene, *Phys. Rev. B* **70**, 132502 (2004).
 - [26] C.C. Homes, R.P.S.M. Lobo, P. Fournier, A. Zimmers, and R. L. Greene, *Phys. Rev. B* **74**, 214515 (2006).
 - [27] I.W. Sumarlin, J.W. Lynn, D.A. Neumann, J.J. Rush, J.L. Peng, Z.Y. Li, and S.J. Hagen, *Physica C* **185-189**, 2571 (1991).
 - [28] S.D. Wilson, P. Dai, S. Li, S. Chi, H.J. Kang, J.W. Lynn, *Nature* **442**, 59 (2006).
 - [29] F. C. Niestemski, S. Kunwar, S. Zhou, S. Li, H. Ding, Z. Wang, P. Dai, V. Madhavan, *Nature* **450**, 1058 (2007).
 - [30] P. B. Allen and B. Mitrovic, in *Solid State Physics*, vol 37, 1 (1982).
 - [31] E. Maiser, P. Fournier, J. L. Peng, F. M. Araujo-Moreira, T. Venkatesan, R. L. Greene, and G. Czjzek, *Physica C* **297**, 15 (1998).
 - [32] M. Beck *et al.*, *Opt. Express* **18**, 9251 (2010).
 - [33] M. Beck, *et al.*, *Phys. Rev. Lett.* **110**, 267003 (2013).
 - [34] see Supplemental Material at <http://link.aps.org/supplemental/xxx>
 - [35] J. P. Hinton, J. D. Koralek, G. Yu, E. M. Motoyama, Y. M. Lu, A. Vishwanath, M. Greven, and J. Orenstein, *Phys. Rev. Lett.* **110**, 217002 (2013).
 - [36] H. Balci, and R.L. Greene, *Phys. Rev. B* **70**, 140508(R) (2004).
 - [37] W. Nessler, S. Ogawa, H. Nagano, H. Petek, J. Shimoyama, Y. Nakayama, and K. Kishio, *Phys. Rev. Lett.* **81**, 4480 (1998).
 - [38] S. Dal Conte, *et al.*, *Nature Physics* **11**, 421–426 (2015)